Available online at www.sciencedirect.com
SCIENCE DIRECT
Polymer 46 (2005) 12016–12025
polymer
www.elsevier.com/locate/polymer

Epoxy nanocomposites with octa(propylglycidyl ether) polyhedral oligomeric silsesquioxane

Yonghong Liu [a], Sixun Zheng [a,*], Kangming Nie [b]

[a] Department of Polymer Science and Engineering, Shanghai Jiao Tong University, 800 Dongchuan Road, Shanghai 200240, China
[b] Department of Materials Science and Engineering, Anhui University, Hefei 230039, People's Republic of China

Received 25 May 2005; received in revised form 9 September 2005; accepted 13 September 2005
Available online 6 October 2005

Abstract

The POSS-containing nanocomposites of epoxy resin were prepared via the co-curing reaction between octa(propylglycidyl ether) polyhedral oligomeric silsesquioxane (OpePOSS) and the precursors of epoxy resin. The curing reactions were started from the initially homogeneous ternary solution of diglycidyl ether of bisphenol A (DGEBA), 4,4′-Diaminodiphenylmethane (DDM) and OpePOSS. The nanocomposites containing up to 40 wt% of POSS were obtained. The homogeneous dispersion of POSS cages in the epoxy matrices was evidenced by scanning electronic microscopy (SEM), transmission electronic microscopy (TEM) and atomic force microscopy (AFM). Differential scanning calorimetry (DSC) and dynamic mechanical analysis (DMA) showed that at the lower POSS concentrations (<30 wt%) the glass transition temperatures (T_gs) of the nanocomposites almost remained invariant whereas the nanocomposites containing POSS more than 40 wt% displayed the lower T_gs than the control epoxy. The DMA results show that the moduli of the nanocomposites in glass and rubbery states are significantly higher than those of the control epoxy, indicating the nanoreinforcement effect of POSS cages. Thermogravimetric analysis (TGA) indicates that the thermal stability of the polymer matrix was not sacrificed by introducing a small amount of POSS, whereas the properties of oxidation resistance of the materials were significantly enhanced. The improved thermal stability could be ascribed to the nanoscaled dispersion of POSS cages and the formation of tether structure of POSS cages with epoxy matrix.

Keywords: Epoxy resin; Polyhedral oligomeric silsesquioxane; Nanocomposites

1. Introduction

Incorporating well-defined inorganic or organometallic building blocks into organic polymers to afford a variety of new and improved properties continues to be a driven force for the development of new polymeric materials [1–7]. Polyhedral oligomeric silsesquioxanes (POSS) are a class of important inorganic–organic hybrid compounds, which can be the precursors to organic–inorganic nanocomposites [8,9]. The cage-like structures of POSS can allow the construction of the materials with precise control of the nanoarchitecture. POSS reagents, monomers and polymers are emerging as a new chemical technology for the nano-reinforced organic–inorganic hybrids [10–19] and the polymers incorporating POSS are becoming the focus of many studies due to the simplicity in processing and the excellent comprehensive properties of this class of hybrid materials. The typical POSS monomers possess the structure of cube-octameric frameworks with eight organic vertex groups, one or more of which is reactive or polymerizable (Scheme 1). The monofunctionalized POSS monomers [20] can be grafted onto macromolecular chains by co-polymerization or reactive blending [21] whereas the bifunctional POSS monomers will allow one to introduce silsesquioxanes building blocks into macromolecular backbones although it is still a challenge to synthesize scaled quantities of bifunctional POSS monomers efficiently [12,15,22,23]. The higher functionalities of POSS monomers can be used to prepare POSS-containing thermosetting nanocomposites [24–29].

Epoxy resins are a class of important thermosetting polymers, which have been widely used as high performance materials, adhesives, matrices of composite materials and electronic encapsulating materials due to their high modulus and strength, excellent chemical resistance and simplicity in processing. The modification of epoxy resin via POSS could endow the materials with some superior properties such as

* Corresponding author. Tel.: +86 21 54743278; fax: +86 21 54741297.
E-mail address: szheng@sjtu.edu.cn (S. Zheng).

0032-3861/$ - see front matter © 2005 Elsevier Ltd. All rights reserved.
doi:10.1016/j.polymer.2005.09.056

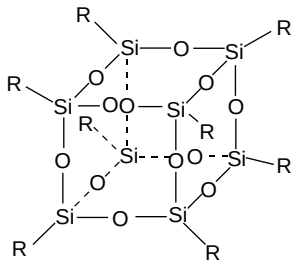

Scheme 1. Structure of polyhedral oligomeric silsesquioxanes.

increased thermomechanical properties, thermal and oxidative stability and dielectric properties (e.g. low dielectric constant) [24,25,27,30–41]. Lee and Lichtenhan [30] reported that the molecular level reinforcement provided by the POSS cages could significantly retard the physical aging process of epoxy resin in the glassy state. Laine et al. [24,25,37–40] investigated the modifications of epoxy resin by a series of octasilsesquioxanes with a variety of R groups such as aminophenyl, dimethylsiloxypropylglycidyl ether groups and found that the dynamic mechanical properties, fracture toughness and thermal stability of the epoxy hybrids were closely dependent on the types of R groups, tether structures between epoxy matrices and POSS cages and the defects in silsesquioxane cages etc. Williams et al. [33] reported that a primary liquid–liquid phase separation occurred at the time of adding the POSS-diamine precursors to epoxy due to the incompatibility between epoxy and isobutyl POSS glycidyl. Matejka et al. [34,35] investigated the structure and properties of epoxy networks reinforced with POSS and the effects of POSS–POSS interactions on the thermal properties were addressed. More recently, we [27] reported that the different morphological structures could be formed in the POSS-containing hybrid composites depending on the types of R groups; moreover, the phase-separated composites and nanocomposites could be prepared by adjusting the degrees of reaction between epoxy matrix and POSS macromer [36]. By reviewing the previous studies, it is noted that several octafunctionalized POSS epoxide monomers were synthesized to incorporate with epoxy resin. Laine et al. [24,25,37] compared the properties of 4,4′-diaminodiphenyl methane (DDM)-cured octakis(dimethylsiloxypropylglycidyl ether)silsesquioxane (OG) and octa(ethylcyclohexenyl epoxide)silsesquioxane (OC) with those of control epoxy resin, i.e. the formulation of diglycidyl ether of bisphenol A (DGEBA) with DDM. Chang et al. [29] investigated the curing kinetics between OG and *meta*-phenylenediamine. More recently, He et al. [26] reported the modifications of a commercial resin by OG and octa(dimethylsiloxybutyle epoxide)silsesquioxane (OB), and the thermomechanical properties of the nanocomposites were investigated. Although the nanoreinforcement effects of POSS on polymeric matrices have been observed in many POSS-containing polymer systems, the precise nature and origin of this behavior is still a matter of debate.

In this communication, we report the preparation of the nanocomposites involving epoxy resin and octa(propylglycidyl ether)polyhedral oligomeric silsesquioxane (OpePOSS) (Scheme 2). The goal of this work is to evaluate the effect of nanodispersed POSS cages on thermal behavior of epoxy matrix and in particular the DMA experiments at the low temperature were carried out to investigate the nature and origin of the nanoreinforcement of POSS in polymer system. To the best of our knowledge, the epoxy-based nanocomposites containing OpePOSS have not been reported yet. The morphology and thermal properties of the nanocomposites are addressed based on scanning electronic microscopy (SEM), atomic force microscopy (AFM), transmission electronic microscopy (TEM), differential scanning calorimetry (DSC), dynamic mechanical analysis (DMA) and thermogravimetric analysis (TGA), respectively.

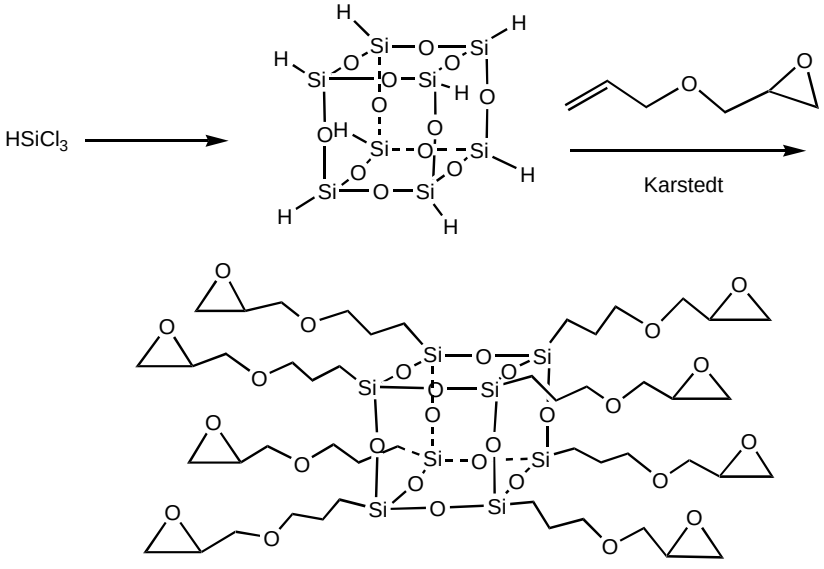

Scheme 2. Syntheses of OpePOSS.

2. Experimental

2.1. Materials

Trichlorosilane ($HSiCl_3$, 98%) was kindly supplied by Shanghai Lingguang Chemical Co., Ltd, China and was used as received. The other chemical reagents, such as ferric chloride ($FeCl_3$), anhydrous $NaHCO_3$, concentrated hydrochloric acid, anhydrous K_2CO_3, $CaCl_2$, allyl glycidyl ether (AGE) and phenol are of chemically pure grade and were purchased from Shanghai Reagent Co., China. Epoxy monomer used, diglycidyl ether of bisphenol A (DGEBA) with a quoted epoxide equivalent weight of 185–210, was purchased from Shanghai Resin Co., China. 4,4′-Diaminodiphenylmethane (DDM) was used as the curing agent, obtained from Shanghai Reagent Co., China.

2.2. Synthesis of octahydrosilsesquioxane ($H_8Si_8O_{12}$)

$H_8Si_8O_{12}$ was synthesized by a modification of the methods described Agaska et al. [43] (Scheme 2). Typically, ferric chloride ($FeCl_3$) (140 g) is dissolved in methanol (200 ml) and the solution was charged to a 5000 ml three-neck round-bottomed flask equipped with a mechanical stirrer. Concentrated HCl (100 ml), petroleum aether (1750 ml) and toluene (250 ml) were added to the system in succession. With vigorously stirring, the mixture of $HSiCl_3$ (100 ml) and petroleum aether (750 ml) was added dropwise by a pressure-equalizing dropping funnel over a period of about 9 h. With an additional 30 min of vigorously stirring, the upper organic layer was transferred to another round-bottom flask. The powder of anhydrous K_2CO_3 (70 g) and anhydrous $CaCl_2$ (50 g) were added with continuously stirring for another 12 h to afford white solids. The solid was filtered out and the solution was concentrated to 50 ml via rotary evaporation. The white crystals (10.3 g) were collected to give a yield of 19.6%. Fourier transform infrared spectroscopy (FTIR) (cm^{-1}, KBr window): 2275 (Si–H); 1121 (Si–O–Si,), 860 (S–H). ^{1}H NMR (chloroform-*d*, ppm): 4.23.

2.3. Synthesis of OpePOSS

The OpePOSS was synthesized via the hydrosilylation reaction between octahydrosilsesquioxane ($H_8Si_8O_{12}$) and allyl glycidyl ether (AGE). In a typical experiment, a 25 ml round-bottom flask pre-filled with 1.0 g $H_8Si_8O_{12}$ and a magnetic bar was dried by the repeated exhausting-refilling process using highly pure nitrogen. Toluene (10 ml) and AGE (3 ml) were charged to the flask and 5 drops of Karstedt catalyst [42] was added with a syringe at ambient temperature. After vigorously stirring for 30 min, the reactive system was heated up to 95 °C and the reaction was allowed to carry out for 36 h to insure the hydrosilylation to completion. The solvent and the excessive AGE were removed under decreased pressure to obtain a viscous liquid. FTIR (cm^{-1}, KBr window): 3056, 2995, 2934, 2873 cm^{-1} (alky C–H); 1255 (C–O–C of epoxide); 1103 (Si–O–Si); 906 (epoxide). ^{1}H NMR (chloroform-*d*, ppm): 3.72–3.42 (m,CH_2O(CH$_2$)$_3$Si–); 3.50–3.35, (m, SiCH$_2$CH$_2$-CH_2O). All the resonance between 3.72 and 3.35 are integrated to be 4.3H). 3.16, (OCH$_2$C*H*, epoxide, 1.0H); 2.79 and 2.60, (CH_2 epoxide, 2.1H); 1.64, (SiCH$_2$CH_2CH$_2$O, 2.5H); 0.62, (SiCH_2CH$_2$CH$_2$O, 2.0H); ^{13}C NMR (chloroform-*d*, ppm): 73.6 (SiCH$_2$CH$_2$*C*H$_2$O); 71.6 (*C*H$_2$O(CH$_2$)$_3$Si); 51.0 (OCH$_2$-*C*H(epoxide); 44.4 (*C*H$_2$ (epoxide)); 23.1 (SiCH$_2$*C*H$_2$CH$_2$O); 8.2 (Si*C*H$_2$CH$_2$CH$_2$O). ^{29}Si NMR (chloroform-*d*, ppm): −65.2 (α addition); −67.6 (β addition small). MALD-TOF-MS spectroscopy (product + Na^+): 1359.1 Da.

2.4. Preparation of nanocomposites

The desired amount of DGEBA and OpePOSS was mixed at 70 °C with continuously stirring for sufficiently long time until the homogeneous solutions were obtained. The curing agent, DDM was then added into the mixture with vigorously stirring until the systems became transparent and homogeneous. The mixtures were poured into Teflon moulds, which were highly polished. The samples were cured at 80 °C for 2 h and 150 °C for 2 h together with a post cure at 180 °C for 2 h to attain the complete curing reaction, which was evidenced by the disappearance of the infrared band at 915 and 835 cm^{-1} that were characteristic of epoxy compounds.

2.5. Measurement and techniques

2.5.1. Fourier transform infrared spectroscopy (FTIR)

The FTIR measurements were conducted on a Perkin–Elmer Paragon 1000 Fourier transform spectrometer at room temperature (25 °C). The samples of the nanocomposites were granulated and the powder was mixed with KBr pellets to press into the small flakes. The specimens were sufficiently thin to be within a range where the Beer–Lambert law is obeyed. In all cases 64 scans at a resolution of 2 cm^{-1} were used to record the spectra.

2.5.2. Matrix-assisted ultraviolet laser desorption/inonization time-of-flight mass spectroscopy (UV-MALDI-TOF-MS)

Gentisic acid (2,5-dihydroxybenzoic acid, DHB) was used as the matrix with tetrahydrofuran as the solvent. The MALDI-TOF-MS experiment was carried out on an IonSpec HiR-esMALDI mass spectrometer equipped with a pulsed nitrogen laser ($\lambda = 337$ nm; pulse with = 3 ns). This instrument operated at an accelerating potential of 20 kV in reflector mode. Sodium is used as the cationizing agent and all the data are shown for positive ions.

2.5.3. Nuclear magnetic resonance spectroscopy (NMR)

The NMR measurement was carried out on a Varian Mercury Plus 400 MHz NMR spectrometer at 27 °C. The samples were dissolved with deuteronated chloroform. The ^{1}H, ^{13}C and ^{29}Si spectra were obtained with tetramethylsilane (TMS) as the reference.

2.5.4. Scanning electronic microscopy (SEM)

To investigate the morphology of POSS-containing epoxy hybrids, the samples were fractured under cryogenic condition using liquid nitrogen. The fractured surfaces were immersed in chloroform at room temperature for 30 min. If the POSS-rich phase were separated out during the in situ polymerization, it could be preferentially etched by the solvent while epoxy matrix phase remains unaffected. The etched specimens were dried to remove the solvents. The fracture surfaces were coated with thin layers of gold of about 100 Å. All specimens were examined with a Hitachi S210 scanning electron microscope (SEM) at an activation voltage of 15 kV.

2.5.5. Atomic force microscopy (AFM)

The AFM experiments were carried out in both height and phase contrast modes using a Digital Instruments Dimension 3000 scanning force microscope in a taping mode. Etched silicon tips on a cantilever (Nanoprobe) with spring constants ranging between 40.0 and 66.0 N/m were used. To investigate the morphology of POSS-containing epoxy hybrids, the samples were fractured under cryogenic condition using liquid nitrogen and the smooth fractured surfaces so obtained were used for morphological observation.

2.5.6. Transmission electronic microscopy (TEM)

The transmission electron microscopy (TEM) was performed on a JEM 2010 high-resolution transmission electron microscope at the accelerating voltage of 120 kV. The samples were trimmed using an ultramicrotome and the specimen sections (c.a. 70 nm in thickness) were placed in 200 mesh copper grids for observation.

2.5.7. Differential scanning calorimetry (DSC)

The calorimetric measurement was performed on a Perkin–Elmer Pyris-1 differential scanning calorimeter in a dry nitrogen atmosphere. The instrument was calibrated with standard Indium. All the samples (about 10 mg in weight) were heated from 20 to 250 °C and the DSC curves were recorded at a heating rate of 20 °C/min. The glass transition temperature was taken as the midpoint of the capacity change.

2.5.8. Dynamic mechanical analysis (DMA)

The dynamic mechanical tests were carried out on a Dynamic Mechanical Thermal Analyzer (DMTA) (MKIII, Rheometric Scientific, Ltd Co., UK) with the temperature range from −130 to 250 °C. The frequency used is 1.0 Hz at the heating rate 5.0 °C/min. The specimen dimension was $1.2\times2\times0.1$ cm^3.

2.5.9. Thermogravimetric analysis (TGA)

A Perkin–Elmer thermal gravimetric analyzer (TGA-7) was used to investigate the thermal stability of the nanocomposites. The samples (about 10 mg) were heated in air atmosphere from ambient temperature to 800 °C at a heating rate of 20 °C/min. The thermal degradation temperature was taken as the onset temperature at which 5 wt% of weight loss occurs.

3. Results and discussion

3.1. Formation of POSS-containing nanocomposites

The hydrosilylation between $H_8Si_8O_{12}$ and allyl glycidyl ether (AGE) was employed to synthesize the target product, octa(propylglycidyl ether)polyhedral oligomeric silsesquioxane (OpePOSS), which was depicted in Scheme 2. The results

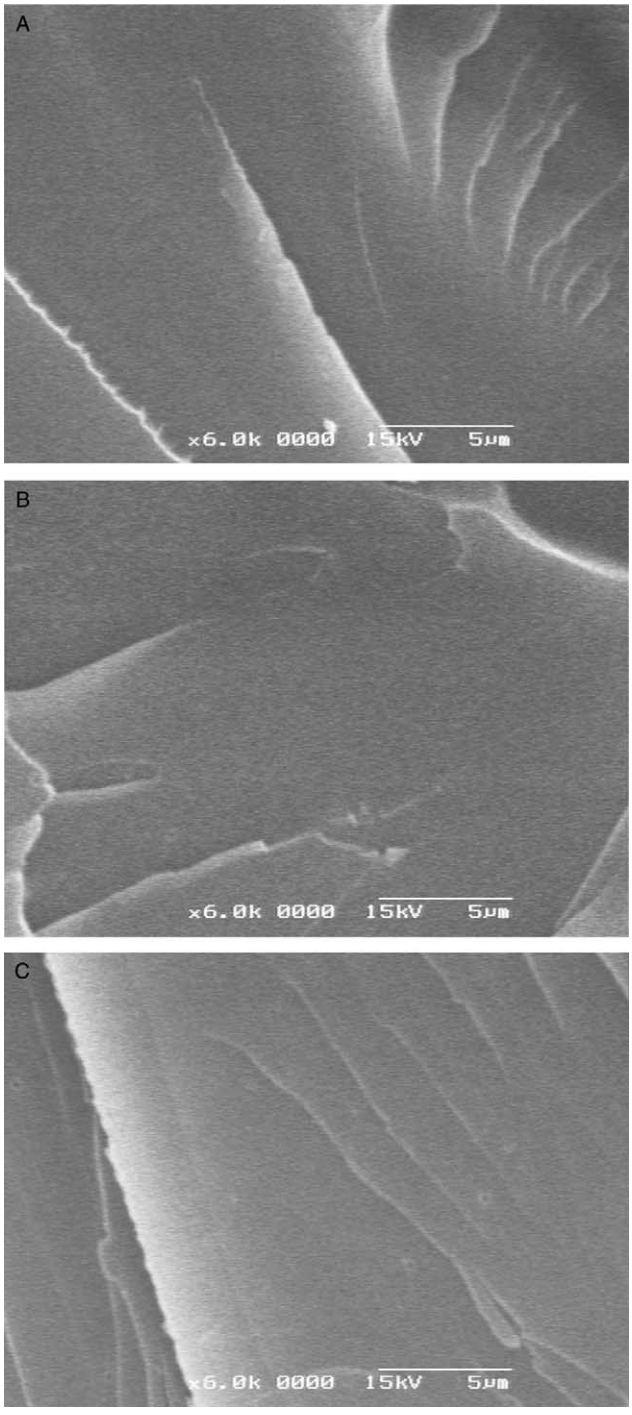

Fig. 1. SEM micrographs: (A) the control epoxy; (B) the unetched nanocomposites containing 40 wt% of POSS; (C) the nanocomposites containing 40 wt% of POSS etched with chloroform for 30 min.

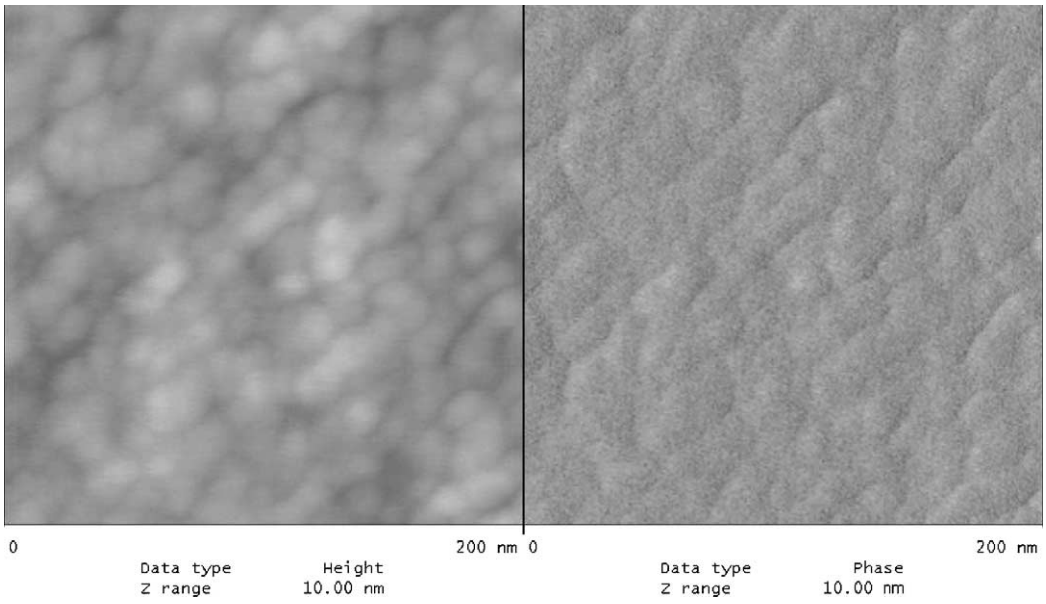

Fig. 2. AFM images of the nanocomposites containing 40 wt% of POSS. Left, height images; Right, phase contrast.

of FTIR, ^{1}H, ^{13}C, ^{29}Si NMR together with MALDI-TOF-MS spectroscopy indicate that OpePOSS was successfully obtained. The octafunctional POSS monomer was employed to prepare the POSS-containing nanocomposites. The POSS-containing nanocomposites were prepared via the in situ curing reaction between DGEBA and DDM in the presence of OpePOSS. It was observed that the ternary mixtures composed of DGEBA, DDM and OpePOSS at the compositions investigated were homogenous. All the cured hybrid composites are transparent, indicating that no phase separation occurred at least on the scale more than the wavelength of visible lights. The morphology of the POSS-containing hybrids was further investigated by means of scanning electronic microscopy (SEM), atomic force microscopy (AFM), transmission electronic microscopy (TEM).

Shown in Fig. 1(B) and (C) are the SEM micrographs of the fracture surfaces of the control epoxy and the hybrids containing 40 wt% of POSS frozen under cryogenic condition using liquid nitrogen. Before and after etched with chloroform, the hybrid composites exhibited the featureless morphologies and no discernable phase separation was observed, which are similar to that of the control epoxy (Fig. 1(A)). This observation suggests that OpePOSS has taken part in the formation of crosslinked networks. The surface analysis of the epoxy hybrids was carried out by atomic force microscopy (AFM). A typical AFM height image of the hybrid containing 40 wt% of POSS is presented in Fig. 2 (left). It is seen that the surface appears to be free of visible defects and it is quite smooth. The phase contrast image (Fig. 4 (right)) of the surface shows a homogenous surface, indicating the surface of the fractured ends is compositionally homogenous, i.e. that no localized areas of POSS aggregates could be observed at the nano-scale. Fig. 3 representatively shows the TEM micrograph of the sectioned hybrid containing 40 wt% of POSS. To contrast with the background, the TEM image was taken at the edge of the sectioned hybrid. It is seen that the dark area (the portion of the hybrid) is quite homogenous and no localized domains were detected at this scale, implying that the POSS component was homogenously dispersed in the continuous epoxy matrix at the nanoscale. The results of AFM and TEM further substantiate that the nanocomposites were successfully obtained.

Apart from the curing reaction between DGEBA and DDM, the crosslinking reaction between OpePOSS and DDM could additionally be involved in the composite system. The reactions were schemed in Scheme 3. The Fourier transform infrared spectroscopy (FTIR) was used to examine the degree of curing reaction after the POSS cages were introduced to the systems. Shown in Fig. 4 are the FTIR spectra of DGEBA, the control epoxy and the nanocomposites containing 5, 10, 20, 30 and 40 wt% of POSS. The pure DGEBA is characterized by the

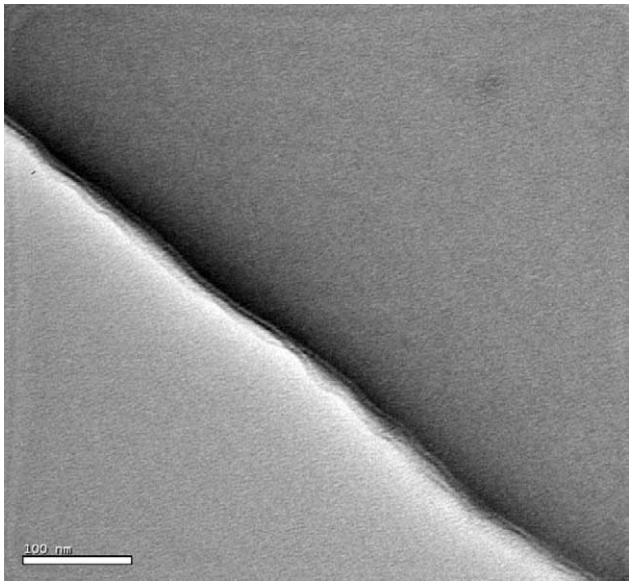

Fig. 3. TEM micrograph of the nanocomposites containing 40 wt% of POSS.

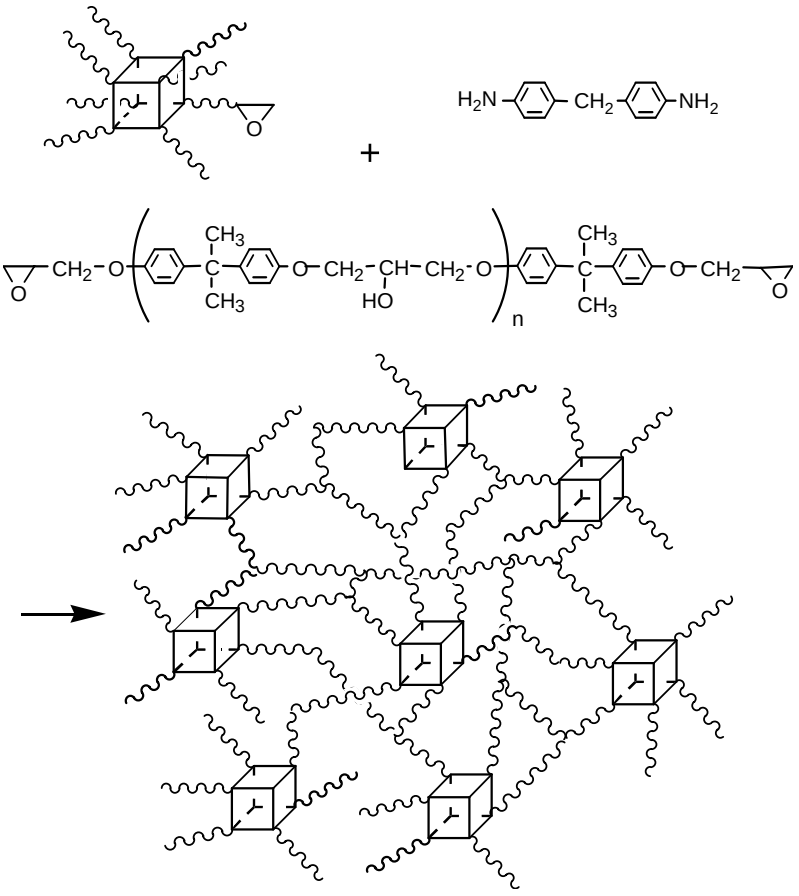

Scheme 3. Preparation of the nanocomposites containing POSS.

stretching vibration band of epoxide groups at 915 cm^{-1} (see curve A). Under the present condition the curing reaction of the control epoxy was quite complete, which was evidenced by the disappearance of the epoxide band (see curve B). It is noted that all the epoxide bands were virtually vanished for the POSS-containing nanocomposites under the identical curing circles, indicating that the curing reactions in the nanocomposites were carried out to completion. In terms of the FTIR results, it is judged that in the POSS-containing hybrids, the epoxy matrices were tightly crosslinked.

3.2. Thermomechanical properties

3.2.1. Glass transitions behavior

The POSS-containing nanocomposites were subject to thermal analysis. The DSC curves of the control epoxy, the nanocomposites are presented in Fig. 5. The control epoxy displayed the glass transition at 175 °C. For the POSS-containing hybrids, all the DSC thermograms displayed single glass transition temperatures (T_gs) in the experimental temperature range (0–210 °C). At the lower concentration (POSS < 40 wt%), the T_gs of the POSS-containing nanocomposites are close to (or slightly lower than) that of the control epoxy. While the POSS content is 40 wt%, the depression of 10 °C in T_gs was found for the nanocomposite. The glass transition behavior was further confirmed by dynamic mechanical analysis (DMA). Shown in Fig. 6 are the plots of DMA tan δ as functions of temperature for the control epoxy and its nanocomposites containing up to 40 wt% of POSS. The dynamic mechanical spectrum of DDM-cured epoxy exhibited a well-defined α relaxation transition centered at 177 °C, which is attributed to the glass transition of the polymer. The dynamic mechanical spectra of all the nanocomposites containing POSS also clearly displayed the single α transitions in the temperature range of −130 to 250 °C. When the content of POSS is less than 40 wt%, the glass–rubber transitions of the nanocomposites occurred at c.a. 177 °C, which is close to that of the control epoxy and the T_g of the nanocomposites containing 10 wt% of POSS was even slightly higher than that of the control epoxy. The DMA results are in a good agreement with those of DSC.

It has been found that the glass transition behavior of POSS-containing nanocomposites is quite dependent on both types of R groups around silsesquioxane cages and the interactions between R groups and polymer matrices. POSS-containing nanocomposites can display the enhanced or reduced glass transition temperatures. For instance, a small amount of POSS loadings gave rise to the significant enhancement of glass transition temperature in cyclopentyl (and/or cyclohexyl) POSS styryl-*co*-4-methyl styrene copolymers. The similar results were also found in other POSS containing hybrids such as poly(norbornene-*co*-norbornene POSS) copolymers [44,45],

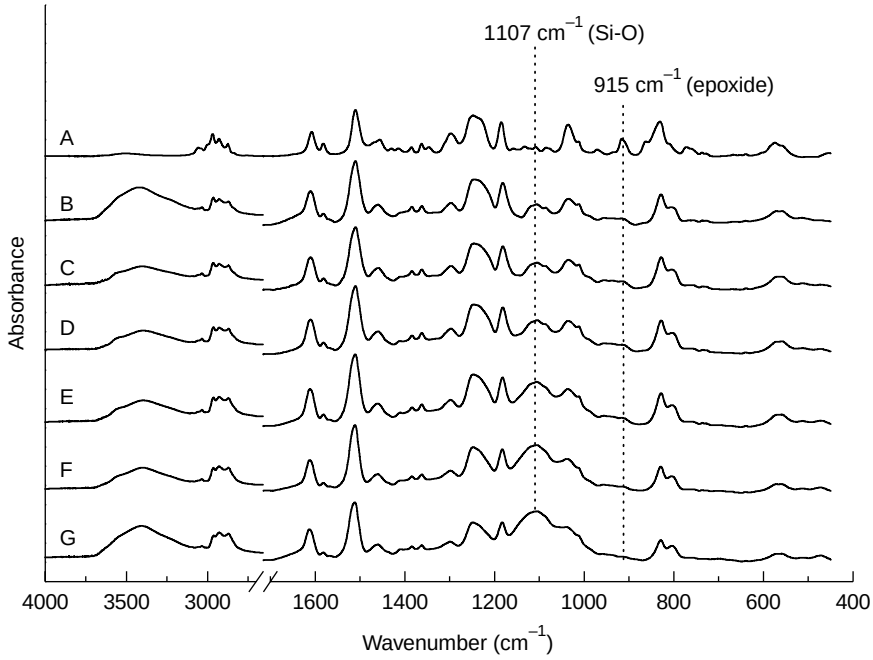

Fig. 4. FTIR spectra: (A) DGEBA, (B) the control epoxy, (C) the nanocomposites containing 5, (D) 10 wt%, (E) 20 wt%, (F) 30 wt% and (G) 40 wt% of OpePOSS.

cyclopentyl POSS containing epoxy resins [30,40]. Nonetheless, it was noted that cyclopentyl POSS containing poly(4-methyl styrene) nanocomposites exhibited the decreased T_gs comparing with the control homopolymers [18]. When the R groups (viz. cyclopentyl) were replaced by cyclohexyls, the counterpart nanocomposites displayed the enhanced T_gs in comparison with the control homopolymers [18]. The decreased T_gs were also reported in several POSS-containing epoxy nanocomposites [27,32,33]. Li and Pittman et al. [32] proposed that the T_g depression could be ascribed to incomplete curing reaction of epoxy due to the inclusion of POSS cages. Nonetheless, the FTIR spectroscopy shows that the curing reactions have performed to completion for the present composite system. In the present case, we noted that the R groups of the POSS molecule are eight aliphatic propyl ether glycidyl groups. The presence of these supple R groups could be responsible for the depression in glass transition temperature for the nanocomposites, which is comparable to the internal plasticization effect [46]. It should be pointed out that in POSS-modified polymer systems, the nanoreinforcement of POSS cages on polymer matrices could restrict the motions of macromolecular chains and thus glass transition temperatures of nanocomposites will be increased. It is worth noticing that only while the POSS content is more than 30 wt%, the nanocomposites displayed the reduced T_gs. The fact that the

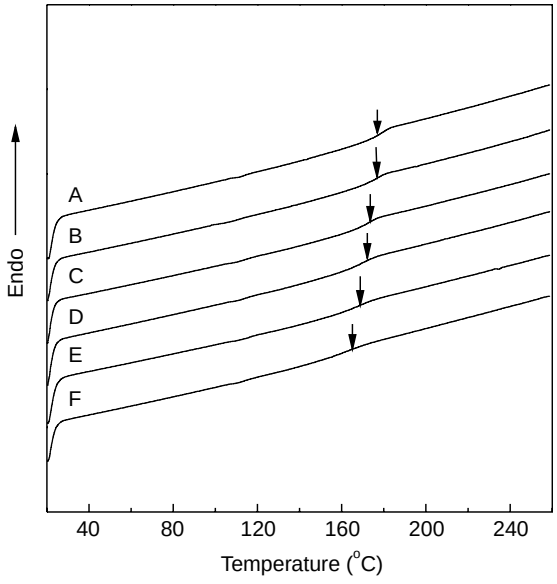

Fig. 5. DSC curves of the control epoxy and its nanocomposites with POSS.

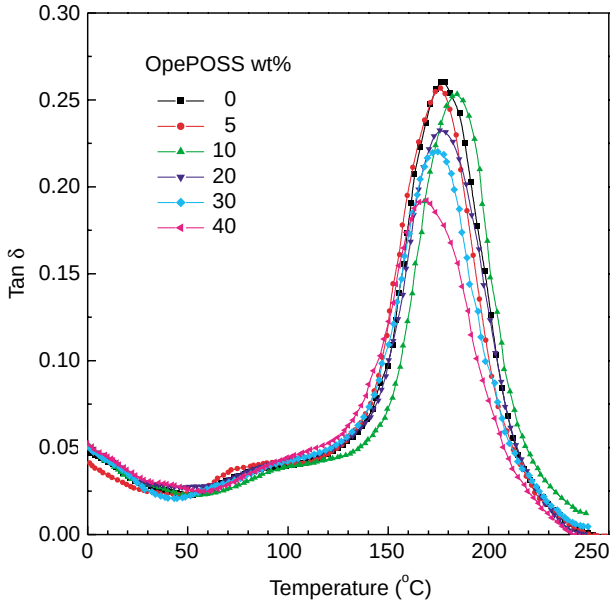

Fig. 6. The plots of DMA tan δ as functions of temperature for the epoxy and nanocomposites in the temperature range of 0–250 °C.

glass transition temperatures of the nanocomposites did not monotonously decrease with increasing the concentration of POSS could suggest that the comprehensive embodiment of the above two factors.

3.2.2. Secondary transitions (β transitions)

In the dynamic mechanical tan δ spectra of epoxy and its nanocomposites with POSS, there exist the low temperature relaxations, commonly referred to as the β transitions, which occurred approximately −50 °C (Fig. 7). The β transition was ascribed to the motion of hydroxyl ether structural unit (–O–CH_2–CH(OH)–CH_2–) and diphenyl groups of the amine-cured epoxy [46–50]. For the present nanocomposite system, it is found that the β transitions obviously splitted into two components while the POSS cages were introduced to system. In comparison with T_β of the control epoxy, one of the two components shifted to the higher temperature (T'_β), whereas the original ones remained unchanged or slightly shifted to the lower temperature. The appearance of the higher-temperature β transition component (i.e. T'_β) implies that the introduction of POSS gives rise to the increased hindrance of motions of macromolecular chains in the crosslinked networks. The difficulty in initiating the crankshaft motion of hydroxyl ether structural units or the motion of diphenyl groups was increased and thus the secondary transition occurred at a relatively higher temperature. This effect could be from the nanoreinforcement of POSS cages. In addition to the effect of reinforcement of POSS, it is in the meantime noted that the other component (T_β) slightly shifted to the lower temperatures with the incorporation of POSS. This observation could be related to the internal plasticization effect of POSS R groups, which facilitates the motion of the hydroxyether structural unit and diphenyl groups. This result is coincident with the observation that that the nanocomposites displayed the decreased glass transition temperatures (T_g) at the higher POSS concentrations. The β

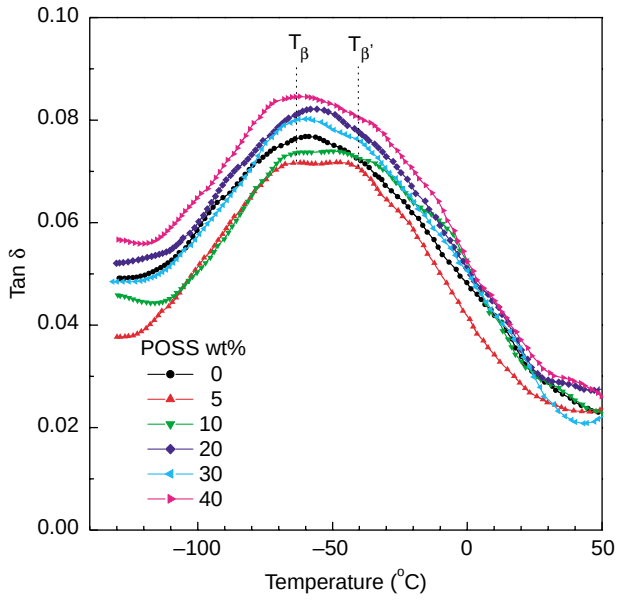

Fig. 7. The plots of DMA tan δ as functions of temperature for the epoxy and nanocomposites in the temperature range of −150 to 50 °C.

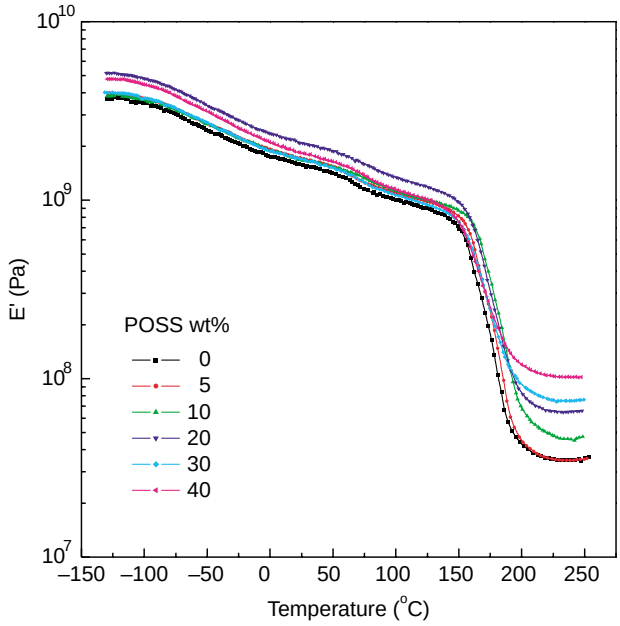

Fig. 8. The plots of DMA dynamic storage moduli as functions of temperature for the control epoxy and its nanocomposites containing POSS.

transition behavior further indicates the simultaneous presence of the opposing effects in POSS-containing nanocomposites.

Dynamic storage modulus shown in Fig. 8 are the plots of storage modulus as functions of temperature for the control epoxy and the nanocomposites with the OpePOSS content up to 40 wt%. It is interesting to note that in the glass state (−50 to 100 °C) the dynamic storage moduli of all the POSS-containing hybrids were significantly higher than that of the control epoxy, and the moduli increased with increasing the concentration of OpePOSS. In the hybrid systems, the POSS cages were homogeneously dispersed in the epoxy matrices on the nanoscale and thus the increased modulus could be attributed to the nanoreinforcement effect of POSS cages on epoxy matrix. Nonetheless, it is noted that the moduli of the nanocomposites did not exhibited the monotonous increment as a function of POSS concentration although all the nanocomposites investigated possessed the increased storage modulus in glassy state. The explanation for this observation could be based on the two opposing effect of POSS cages on the matrices of the materials. On the one hand, the nanoreinforcement effect of cubic silsesquioxane cages on polymer matrix will result in the increased modulus of materials. In addition, the aliphatic R groups of OpePOSS could contribute to the decrease in modulus for the nanocomposites, especially at the higher concentration of OpePOSS. The similar phenomenon was also found in other POSS-containing nanocomposites [29,51,52].

It is also worth noticing that the storage moduli of rubbery plateau for the POSS-containing nanocomposites increased with increasing the concentration of POSS. The moduli of rubber plateau for polymer networks are generally related to the crosslinking density of the materials. In the POSS-containing nanocomposites, the crosslinking densities of materials are expected to be lower than that of the control

epoxy since the massive and bulky POSS cages could take up the crosslinking nodules instead of DGEBA, which will reduce the crosslinking density of the networks. The crosslinking densities will decrease with increasing the concentration of POSS in the nanocomposites. However, it is seen that the storage moduli of the nanocomposites containing POSS are significantly higher than that of the plain epoxy, implying the significant nanoreinforcement of POSS cages, which were covalently bonded with the crosslinking networks of the epoxy resin. In the present case, the nanoreinforcement of POSS cages could be the dominant factor to affect the moduli of the nanocomposites.

3.2.3. Thermal stability

Thermogravimetric analysis (TGA) was applied to evaluate the thermal stability of the POSS-containing nanocomposites. Shown in Fig. 9 are the TGA curves of the control epoxy and the nanocomposites recorded in air atmosphere at 20 °C/min. Within the experimental temperature range, all the TGA curves displayed two-step degradation mechanism, suggesting that the existence of POSS did not significantly alter the degradation mechanism of the matrix polymers. For the control epoxy, the initial decomposition occurred at 410 °C and no ceramic yield was obtained for DDM-cured epoxy as expected. For the nanocomposites, the initial decomposition temperatures remained unchanged while the ceramic yields significantly increased with increasing POSS concentration. In addition, it is also noted that the rates of mass loss from segmental decomposition were significantly decreased for the nanocomposites. In terms of the initial decomposition temperatures and the ceramic yields the thermal stability of the nanocomposites was significantly enhanced with inclusion of the inorganic component.

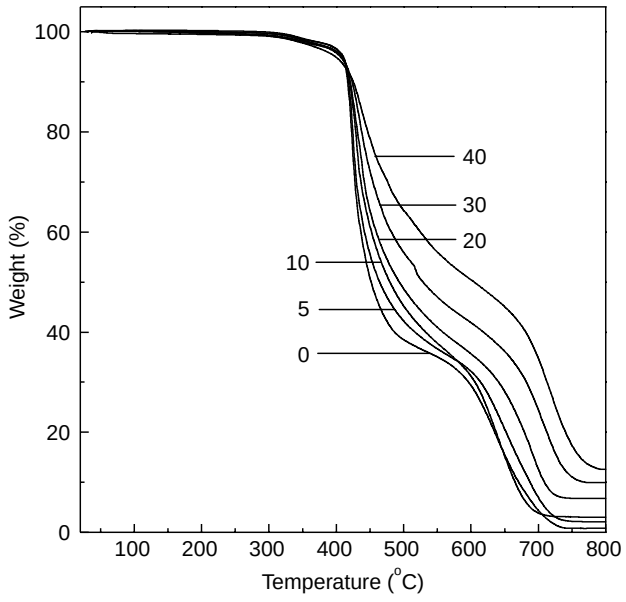

Fig. 9. TGA curves for the control epoxy and its nanocomposites containing POSS, recorded at 20 °C/min in air.

It has been proposed that the tether structure was crucial to improvement in thermal stabilities of POSS-containing nanocomposites [24,25]. In the present case, POSS cages participated in the formation of the crosslinked network, i.e. the POSS cages were tethered onto polymer matrix. In addition, the nanoscaled dispersion of POSS cages in epoxy matrices is an important factor to contribute the enhanced thermal stability. It is plausible to propose that mass loss from segmental decomposition via gaseous fragments could be suppressed by well-dispersed POSS cubes at the molecular level. The similar results were also founded in fully exfoliated polymer–clay nanocomposites [53–56]. Therefore, the improved thermal stability of the nanocomposites could be a result of the combined effects of the formation of tether structure between epoxy matrix and POSS cages and the nanoscaled dispersion of POSS cages in epoxy matrix.

4. Conclusions

The POSS-containing hybrids of epoxy resin were prepared via the co-curing reaction between octa(propylglycidyl ether) polyhedral oligomeric silsesquioxane (OpePOSS) and the precursors of epoxy resin. The curing reactions were started from the initially homogeneous ternary solution of DGEBA, DDM and OpePOSS. The results of transmission electronic microscopy (TEM) and atomic force microscopy (AFM) indicate that the organic–inorganic nanocomposites have successfully been obtained. Differential scanning calorimetry (DSC) and dynamic mechanical analysis (DMA) showed that at the lower POSS concentrations (<40 wt%) the glass transition temperatures (T_g) of the nanocomposites remain almost invariant and the nanocomposites displayed the lower T_gs than the control epoxy at the higher concentration of POSS (e.g. >40 wt%). The DMA results show that the moduli of the nanocomposites in glass and rubbery states are significantly higher than those of the control epoxy, indicating the nanoreinforcement effect of POSS cages. Thermogravimetric analysis (TGA) indicates that the thermal stability of the polymer matrix was not sacrificed by introducing a small amount of POSS, whereas the properties of oxidation resistance of the materials were significantly enhanced. The improved thermal stability could be ascribed to the nanoscaled dispersion of POSS cages and the formation of tether structure of POSS cages with epoxy matrix.

Acknowledgements

This financial support from Shanghai Science and Technology Commission, China under a key project (No. 02DJ14048) was acknowledged. The authors thank the Natural Science Foundation of China (Project No. 20474038 & 50390090) and Shanghai Education Development Foundation, China under an Award (2004-SG-18) to 'Shuguang Scholar' for the partial support.

References

[1] Whitesides GM, Mathias JP, Seto CT. Science 1991;254:1312.
[2] Brinker C, Scherer G. Sol–gel science: the physics and chemistry of sol–gel processing. New York: Academic Press; 1990.
[3] Theng BKG. Developments in soil science. Formation and properties of clay–polymer complexes. vol. 9. Amsterdam: Elsevier; 1979.
[4] Lan T, Kaviratna PD, Pinnavaia TJ. Chem Mater 1995;7:2144.
[5] Giannelis EP. JOM 1992;44:28.
[6] Giannelis EP, Krishnamoorti R, Manias E. Adv Polym Sci 1999;138:107.
[7] Schwab JJ, Lichtenhan JD. Appl Organomet Chem 1998;12:707.
[8] Li G, Wang L, Ni H, Pittman CU. J Inorg Organomet Polym 2001;11:123.
[9] Abe Y, Gunji T. Prog Polym Sci 2004;29:149.
[10] Feher FJ, Wyndham KD, Baldwin RK, Soulivong D, Lichtenhan JD, Ziller JW. Chem Commun 1999;1289.
[11] Feher FJ, Wyndham KD, Soulivong D, Nguyen F. J Chem Soc, Dalton Trans 1999;1491.
[12] Lichtenhan JD, Vu NQ, Carter JA, Gilman JW, Feher FJ. Macromolecules 1993;26:2141.
[13] Lichtenhan JD, Otonari YA, Carr MJ. Macromolecules 1995;28:8435.
[14] Haddad TS, Lichtenhan JD. J Inorg Organomet Polym 1995;5:237.
[15] Mantz RA, Jones PF, Chaffee KP, Lichtenhan JD, Gilman JW, Ismail IMK, et al. Chem Mater 1996;8:1250.
[16] Haddad TS, Lichtenhan JD. Macromolecules 1996;29:7302.
[17] Gilman JW, Schlitzer DS, Lichtenhan JD. J Appl Polym Sci 1996;60:591.
[18] Romo-Uribe A, Mather PT, Haddad TS, Lichtenhan JD. J Polym Sci, Part B: Polym Phys 1998;36:1857.
[19] Zhang C, Laine RM. J Organomet Chem 1996;521:199.
[20] Marcolli C, Calzaferri G. Appl Organomet Chem 1999;13:213.
[21] Zheng S, Feher FJ, Xiao J, Jin R-Z. Polymer nanocomposites, symposium proceeding series, Materials Research Society. vol. 733E 2002.
[22] Lichtenhan JD, Hadddad TS, Schwab JJ, Carr MJ, Chaffee KP, Mather PT. Polym Prepr 1998;39:489.
[23] Wright ME, Schorzman DA, Feher FJ, Jin R-Z. Chem Mater 2003;15:264.
[24] Choi J, Harcup J, Yee AF, Zhu Q, Laine RM. J Am Chem Sci 2001;123:11420.
[25] Choi J, Kim SG, Laine RM. Macromolecules 2004;37:99.
[26] Mya KY, He C, Huang J, Xiao Y, Dai Y, Siow Y-P. J Polym Sci, Part A: Polym Chem 2004;42:3490.
[27] Ni Y, Zheng S. Polymer 2004;45:5557.
[28] Ni Y, Zheng S. Chem Mater 2004;16:5141.
[29] Chen W-Y, Wang Y-Z, Kuo S-W, Huang C-F, Tung P-H, Chang F-C; in press.
[30] Lee A, Lichtenhan JD. Macromolecules 1998;31:4970.
[31] Fu BX, Hsiao BS, White H, Rafailovich M, Mather PT, Jeon HG. Polym Int 2000;49:437.
[32] Li GZ, Wang L, Toghiani H, Daulton TL, Koyama K, Pittman Jr CU. Macromolecules 2001;34:8686.
[33] Abad MJ, Barral L, Fasce DF, Williams RJJ. Macromolecules 2003;36:3128.
[34] Matejka L, Strachota A, Plestil J, Whelan P, Steinhart M, Slaof M. Macromolecules 2004;37:9449.
[35[Strachota A, Kroutilova I, Kovarova J, Matejka L. Macromolecules 2004;38:9457.
[36] Liu H, Zheng S, Nie K. Macromolecules 2005;38:5088.
[37] Laine RM, Choi J, Lee I. Adv Mater 2001;13:800.
[38] Choi J, Yee AF, Laine RM. Macromolecules 2003;36:5666.
[39] Choi J, Tamaki R, Kim SG, Laine RM. Chem Mater 2003;15:3365.
[40] Choi J, Yee AF, Laine RM. Macromolecules 2004;37:3267.
[41] Fu BX, Namani M, Lee A. Polymer 2003;44:7739.
[42] Steffanut P, Osban JA, DeCian A, Fisher J. Chem Eur J 1998;10:2008.
[43] Agaska PA. Inorg Chem 1991;30:2707.
[44] Mather PT, Jeon HG, Romo-Uribe A, Haddad TS, Lichtenhan JD. Macromolecules 1999;32:1194.
[45] Bharadwaj RK, Berry RJ, Farmer BL. Polymer 2000;41:7209.
[46] Ochi M, Okasaki M, Shimbo M. J Polym Sci, Part B: Polym Phys 1982;20:89.
[47] Shiraishi T, Motobe H, Ochi M, Nakanishi Y, Konishi I. Polymer 1992;33:2975.
[48] Sanja ZN, Kupehela L. Polym Eng Sci 1976;28:1149.
[49] Mijovic J, Tsay L. Polymer 1981;22:903.
[50] Shibanov YD, Godovsky YK. Prog Colloid Polym Sci 1989;80:110.
[51] Leu C-M, Reddy M, Wei K-H, Shu C-F. Chem Mater 2004;15:2261.
[52] Leu C-M, Chang Y-T, Wei K-H. Chem Mater 2004;15:3271.
[53] Pebaron PC, Wang Z, Pinnavaia TJ. Appl Clay Sci 1999;15:1.
[54] Ray SS, Okamoto M. Prog Polym Sci 2003;28:1539.
[55] Hergenrother PM, Thompson CM, Smith JG, Connell JW, Hinkley JA, Lyon RE, et al. Polymer 2005;46:5012.
[56] Liu H, Zhang W, Zheng S. Polymer 2005;46:157.